JOURNAL OF MATERIALS SCIENCE 40 (2005) 733–740

Hot rolling workability, texture and grain boundary character distribution of B2-type FeAl, NiAl and CoTi intermetallic compounds

Y. KANENO*, T. YAMAGUCHI, T. TAKASUGI
Department of Metallurgy and Materials Science, Graduate School of Engineering, Osaka Prefecture University, 1-1 Gakuen-cho, Sakai, Osaka 599-8531, Japan
E-mail: kaneno@mtl.osakafu-u.ac.jp

Hot-rolling workability, texture and grain boundary character distribution of B2-type FeAl, NiAl and CoTi intermetallic compounds were investigated as a function of alloy stoichiometry. All the FeAl (i.e., Fe-38Al, -43Al and -48Al, denoted by at.%), and stoichiometric NiAl and CoTi were successfully hot-rolled at 1273 K but off-stoichiometric NiAl (Ni-48Al and -52Al) and CoTi (Co-48Ti and -49Ti) failed. After hot-rolling, all the FeAl showed microstructures with recrystallized coarse grains while (stoichiometric) CoTi retained a deformed microstructure. Hot-rolled (stoichiometric) NiAl showed an intermediate microstructure between FeAl and CoTi. The hot-rolling and annealing textures of FeAl essentially consisted of {111}⟨u v w⟩. For NiAl and CoTi, {111}⟨110⟩ and {111}⟨112⟩ were prominent in the hot-rolling texture, respectively. Both the hot-rolled NiAl and CoTi showed fully-recrystallized microstructures by subsequent annealing, but the resultant recrystallization textures were similar to their hot-rolling textures. On the other hand, grain boundary character distributions of FeAl, NiAl and CoTi with fully-recrystallized microstructures were similar to one another and characterized by a high frequency of low angle boundaries (i.e. $\Sigma 1$ boundaries). Based on these results, recrystallization and grain boundary structure of the B2-type ordered intermetallic compounds were briefly discussed.

1. Introduction

Many B2-type intermetallic compounds have been considered to possess potential as high temperature structural materials. In particular, B2-type FeAl and NiAl have been widely studied from not only fundamental but also practical view of point, because these intermetallic compounds show good corrosion and/or sulfidizing resistance at elevated temperatures and are low cost and low density. On the other hand, B2-type CoTi has its solid solution range from 50 at.% to 55 at.% Co and is stable up to its melting point (∼1600 K) [1, 2]. CoTi is known to show a positive temperature dependence of yield strength [3]. Recently, the present authors have reported that stoichiometric CoTi shows a limited but distinctive tensile plastic elongation at room temperature by means of improving microstructure [4]: (i) deformed microstructure, i.e. introduction of lattice defects such as dislocations and vacancies, (ii) grain refining and (iii) modification of grain morphology. These microstructural modifications have been beneficial to not only intrinsic room-temperature tensile properties but also extrinsic one (i.e., moisture-induced embrittlement) of CoTi.

In general, B2-type intermetallic compounds as well as many other intermetallic compounds show poor ductility at room temperature but they can be plastically deformed at elevated temperatures. Actually, FeAl [5–7], NiAl [8] and CoTi [9] have been reported to be hot-worked by conventional extrusion or rolling. For the fabrication of structural materials, workability is one of the important concerns. Moreover, resultant microstructures such as grain size, crystallographic texture and grain boundary structure are also of importance because these factors affect the mechanical properties of materials.

The textures of plastically deformed FeAl [10] including (imperfectly B2 or $D0_3$) Fe_3Al [11–14] and NiAl [15] have been reported but those of CoTi have not been investigated so far. In the present study, B2-type FeAl, NiAl and CoTi intermetallic compounds were hot rolled and subsequently annealed to investigate hot-workability, texture and grain boundary character distribution as a function of alloy stoichiometry. The main purpose of this paper is to provide fundamental information for microstructure development of monolithic (binary) B2-type intermetallic compounds during hot-rolling and recrystallization.

*Author to whom all correspondence should be addressed.

2. Experimental procedures

Three kinds of B2-type FeAl, NiAl and CoTi with different chemical compositions, i.e., Fe-38Al, -43Al and -48Al, Ni-48Al, -50Al and -52Al, and Co-48Ti, -49Ti and -50Ti (denoted by at.%) were used in this study. Purity of each raw material used was 99.9 wt%. All the compounds were prepared by arc melting in an argon gas atmosphere on a copper hearth using non-consumable tungsten electrode. Homogenization heat treatment was conducted in a vacuum at 1373 K for 24 h (FeAl), at 1323 K for 48 h (NiAl) and at 1473 K for 48 h (CoTi), respectively, followed by furnace cooling. Homogenized ingot with a thickness of ∼10 mm was sheathed with stainless steel, and then hot-rolled at 1273 K in air to ∼80% reduction. Hot-rolling was conducted by a laboratory roll with a roll diameter of 120 mm using an average draught of 0.1 mm. The rolled material was heated every one pass. Recrystallization annealing for the hot-rolled sheet was conducted in a vacuum at 1273 K for 10 h, followed by furnace cooling at a cooling rate of ∼600 K/h. No vacancy elimination treatment was carried out for all the compounds in this study. For microhardness measurement, more than ten points were measured using mainly a load of 200 g. For macrotexture, conventional X-ray pole figures were measured using samples with a size of $\sim 20 \times 20$ mm^2. The measured {110} and {200} pole figure data were corrected by using the randomly oriented powder sample. For microtexture including grain boundary structure, local orientations were measured by the electron backscatter diffraction (EBSD) technique using the same samples as those for the X-ray pole figure measurement. Typically, the area of $\sim 3 \times 3$ mm^2 was scanned and the total points of ∼55000 were analyzed using the INCA Crystal^{TM} software developed by OXFORD INSTRUMENTS. The Brandon criterion [16]: $\Delta\theta_{max} = 15^\circ \Sigma^{-1/2}$ was used to classify the grain boundary character in terms of the coincidence site lattice (CSL) model.

3. Results and discussion

3.1. Hot-rolling behavior

Fig. 1 shows the appearance of the hot-rolled sheets after removing a stainless steel sheath. All the FeAl (i.e., Fe-38Al, -43Al and -48Al) were successfully hot-rolled at 1273 K although edge cracking somewhat occurred in all the compounds. On the other hand, hot rolling behavior of NiAl and CoTi strongly depends on alloy stoichiometry. Stoichiometric NiAl (Ni-50Al) and CoTi (Co-50Ti) were successfully hot-rolled but off-stoichiometric NiAl (Ni-48Al and -52Al) and CoTi (Co-48Ti and -49Ti) failed.

Microhardness of as-homogenized (unrolled), hot-rolled and annealed compounds are shown in Fig. 2. Fig. 2 clearly indicates that for the measured three kinds of intermetallic compounds, hardness is strongly dependent on alloy stoichiometry but not so much dependent on the fabricated state. For FeAl, hardness increases with increasing Al content. All the FeAl used in this study are off-stoichiometric. In this case, the degree of ordering is assumed to decrease with decreasing Al content, and possibly Fe-38Al is more disordered (alloy-like) than Fe-48Al. Fe-48Al shows the highest hardness among all the compositions investigated in this study. It is also interesting to note in this figure that the hardness is little sensitive to the fabricated state (i.e., as-homogenized, the hot-rolled and annealed

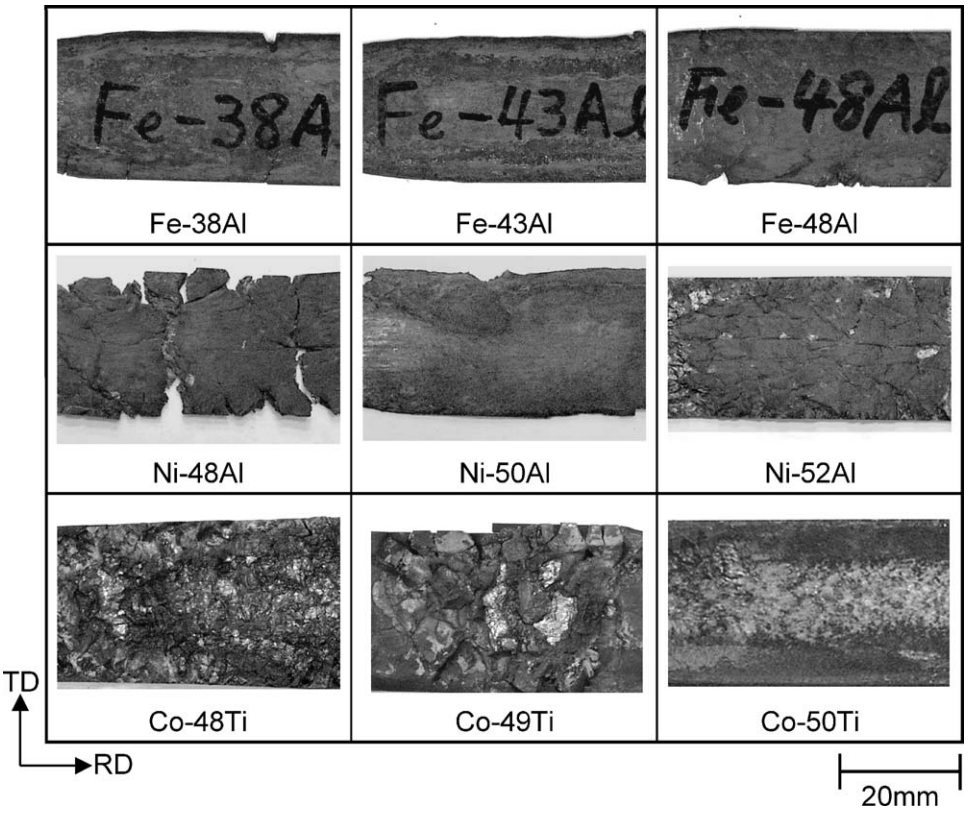

Figure 1 Appearance of the hot-rolled FeAl, NiAl and CoTi sheets.

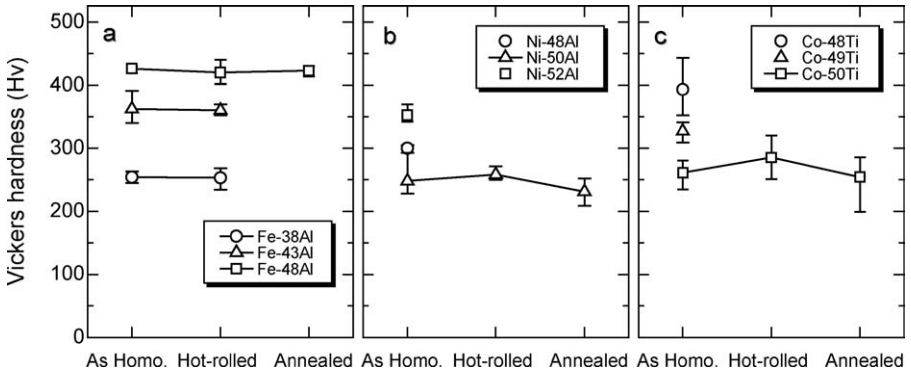

Figure 2 Vickers microhardness of: (a) FeAl, (b) NiAl and (c) CoTi in the as-homogenized (unrolled), hot-rolled and annealed (1273 K–10 h) states, respectively.

states). For NiAl, a stoichiometric compound shows lower hardness than off-stoichiometric compounds. In addition, Al-rich NiAl (Ni-52Al) shows higher hardness than Ni-rich NiAl (Ni-48Al). It is well known that defect structure of NiAl strongly depends upon alloy stoichiometry: the defect structure of Al-rich NiAl is vacancy-type while that of Ni-rich NiAl is anti-site-type [17], and a hardness increase with deviation from stoichiometry is larger in Al-rich side than in Ni-rich side. This indicates that stoichiometric NiAl is *soft* while off-stoichiometric NiAl is *hard*. In fact, only the stoichiometric NiAl was successfully hot-rolled at 1273 K. Also, it is noted that the hardness of the stoichiometric NiAl is little changed by either hot-rolling or annealing. For CoTi, a stoichiometric compound is softer than off-stoichiometric compounds. As Ti content deceases, the hardness increases due to anti-site-type structure involved in the Co-rich composition [2]. Only stoichiometric CoTi was consequently hot-rolled, similar to the hot-rolling of NiAl. For NiAl and CoTi, the defect structures introduced by deviation from the stoichiometry possibly affect the nature or movement of dislocations, resulting in the striking hardening and poor workability.

3.2. Optical microstructure

Fig. 3 shows optical micrographs of Fe-48Al, Ni-50Al and Co-50Ti which were hot-rolled and subsequently annealed at 1273 K for 10 h, respectively. Hot-rolled Fe-48Al shows a microstructure with recrystallized coarse grains, indicating that recrystallization occurred during the hot-rolling process. The other FeAl alloys (i.e., Fe-38Al and -43Al) also showed a similar microstructure with Fe-48Al. After annealing at 1273 K for 10 h, grain growth occurred in FeAl. On the contrary, hot-rolled Co-50Ti retained the deformed microstructure. This corresponds to the hardness increase by hot-rolling (Fig. 2c). Hot-rolled Ni-50Al shows an intermediate microstructure between hot-rolled Fe-48Al and Co-50Ti, i.e., partially retained the deformed microstructure. After annealing at 1273 K for 10 h, both Co-50Ti and Ni-50Al show fully recrystallized microstructures. Grain size of annealed Ni-50Al is larger than that of

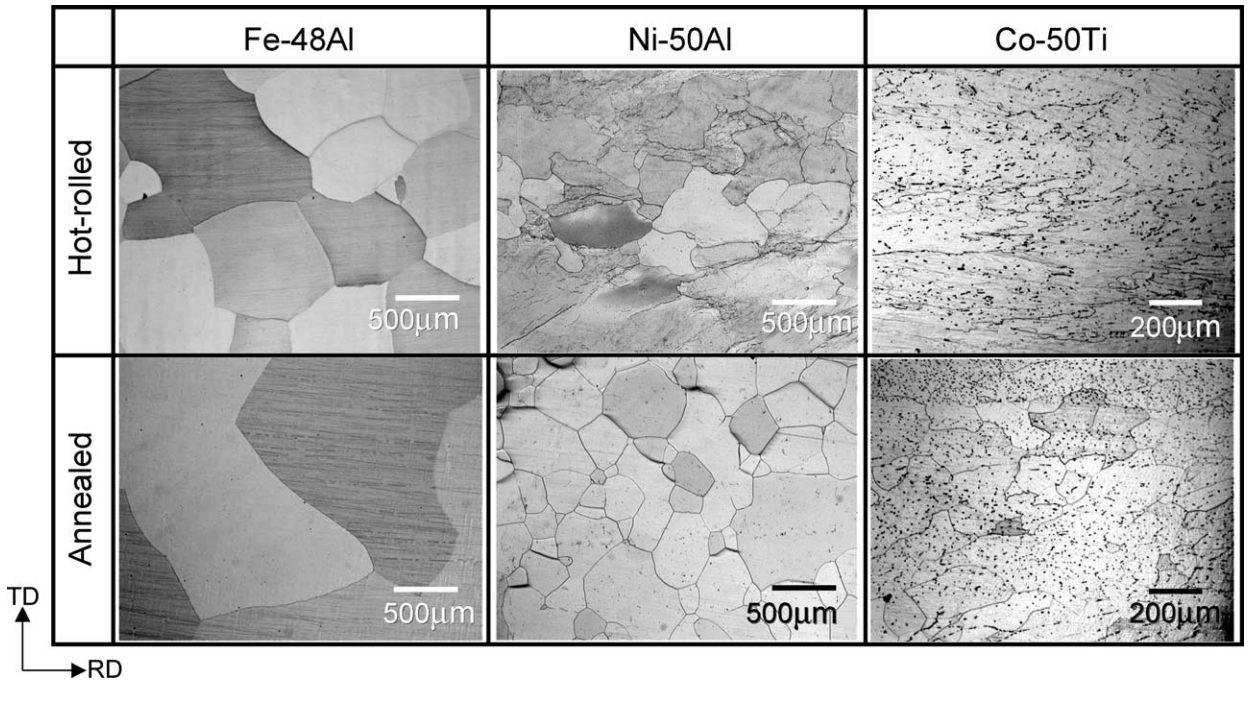

Figure 3 Optical micrographs of Fe-48Al, Ni-50Al and Co-50Ti hot-rolled and subsequently annealed at 1273 K for 10 h. RD and TD indicate rolling and transverse directions, respectively.

annealed Co-50Ti. Fig. 3 suggests that recrystallization during hot-rolling process occurs easily in the order of FeAl, NiAl and CoTi. For FeAl, good workability is probably associated with easy recrystallization during hot-rolling process.

Generally describing, recrystallization temperature of material is estimated to occur at $\sim 0.5T_m$(T_m: melting temperature) though it strongly depends on purity of material and degree of deformation. Melting points are 1911 K for NiAl, 1598 K for CoTi and 1583 K for FeAl, respectively. Therefore, it is considered that recrystallization temperature of FeAl is lowest among the compounds used in the present study. In fact, fully recrystallized microstructure was formed during hot-rolling of FeAl, primarily consistent with this prediction. More strictly describing, recrystallization is related to diffusion process. Interdiffusion coefficients in FeAl (Fe-47Al), NiAl (Ni-47Al) and CoTi (Co-50Ti) have been reported to be in the range of $\sim 10^{-13}$ [18], $\sim 10^{-16}$ [18] and 10^{-16} [19] m^2s^{-1} at $\sim$1273 K, respectively. Therefore, an idea based on the diffusion coefficient predicts that recrystallization involving grain growth process (i.e., diffusion process) occurs more easily in FeAl than in NiAl and CoTi, consistent with the experimental result observed in this study. In the meantime, it has been reported that many B2-type intermetallic compounds contain a high density of thermal vacancies and that these vacancies strongly affect high-temperature properties relating to the diffusion process. Actually, relatively high density of thermal vacancies have been reported to be easily introduced in FeAl and NiAl [20–22]. However, it has been assumed that CoTi does not contain a high density of thermal vacancies in comparison with FeAl and NiAl [9]. Consequently, it is easily suggested that the diffusion-related process including recrystallization is slower in CoTi than in NiAl as well as in FeAl. Thus, it is suggested that the diffusion process, which is largely affected by thermal vacancies, dominates the present recrystallization behavior during hot-rolling process.

Furthermore, there may be another factor affecting recrystallization of ordered intermetallic compounds. Ordering energy (or anti-phase boundary (APB) energy) may affect the recrystallization of ordered intermetallic compounds. Ordering energy of NiAl and CoTi is supposed to be higher than that of FeAl. For the ordered intermetallic compounds, the degree of order is reduced by rolling deformation. In the subsequent recrystallization process, reordering possibly affects recovery process (i.e., annihilation and rearrangement of dislocations). Therefore, it is possible that recrystallization of NiAl and CoTi with high ordering energy is retarded by reordering in comparison with FeAl with low ordering energy.

3.3. Hot-rolling and annealing textures

Initial textures of the homogenized ingots (i.e., starting materials before the hot-rolling) showed mostly a single orientation, which was different by the ingot. Fig. 4 shows {100} pole figures of Fe-48Al, Ni-50Al and Co-50Ti which were hot-rolled and subsequently annealed at 1273 K for 10 h, respectively. In Fig. 4, the pole figures of Fe-48Al show a summed texture of pole figures taken from three different areas. Hot-rolling texture of Fe-48Al seems to be fairly random but consists mainly of orientations with a {111} plane parallel to the surface of the sheet (i.e., {111}⟨uvw⟩). Similar texture was observed for Fe-38Al and -43Al. For hot-rolled Ni-50Al and Co-50Ti, {111}⟨110⟩ and {111}⟨112⟩ orientation were prominently formed, respectively. Annealing textures of all the compounds are dispersed but are still composed of orientations similar to those of the

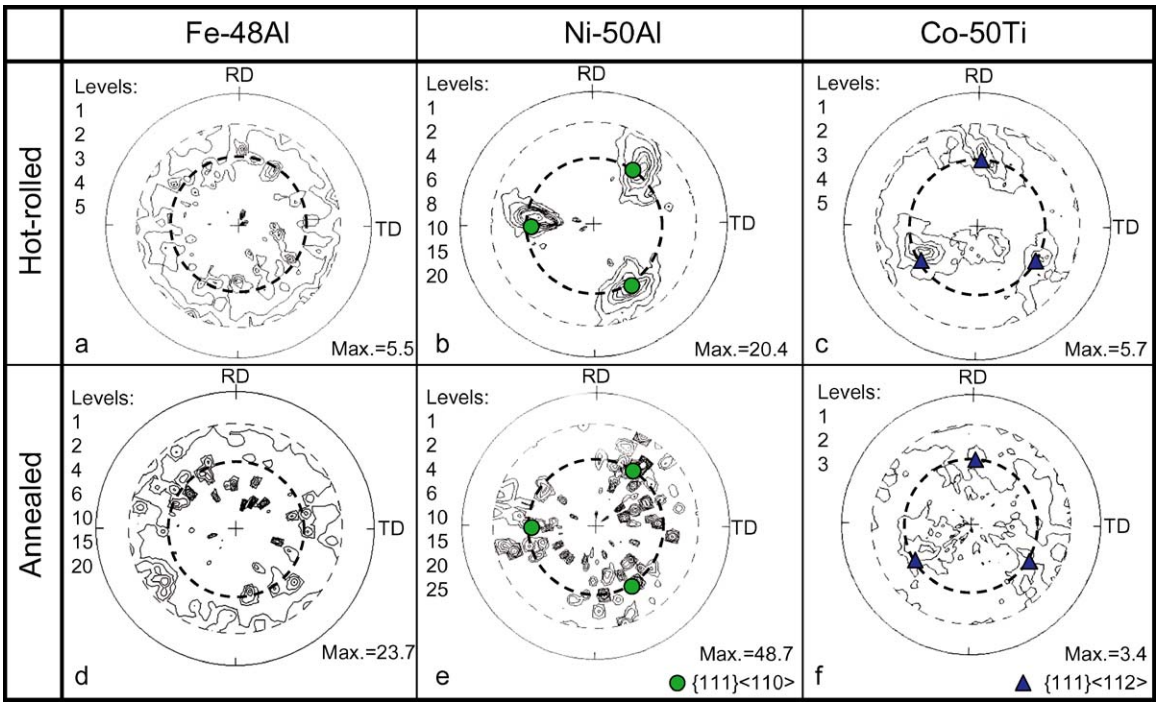

Figure 4 {100} pole figures showing: (a–c) hot-rolling and (d–f) annealing textures of Fe-48Al, Ni-50Al and Co-50Ti.

hot-rolling texture. For NiAl as well as FeAl, the intensified annealing textures accompanied with discrete orientation distribution are possibly due to large grain size, and therefore insufficiently collected data. In the case of Fe-48Al, the annealing texture is possibly associated with (abnormal) grain growth.

In rolled disordered bcc materials such as iron and low carbon steels, two types of fiber texture components are developed. One is the α-fiber which comprises orientations with a common crystallographic ⟨110⟩ direction parallel to the rolling direction (RD): in the α-fiber, {001}⟨110⟩, {112}⟨110⟩ and {111}⟨110⟩ exist as major components [23]. Another is the γ-fiber which contains all orientations with a {111} plane parallel to the surface of the sheet, including {111}⟨110⟩ and {111}⟨112⟩ orientations as major components [23]. In general, the intensity of the α-fiber components decreases while that of the γ-fiber components remains constant or increases during annealing [24]. Basically, the observed hot-rolling and annealing textures of the present compounds are consistent with those of the disordered bcc materials.

Deformation texture is formed by crystal lattice rotation due to slip deformation. It is known that slip system for B2-type FeAl is ⟨100⟩{011} at temperatures above 0.4 Tm though ⟨111⟩{011} slip system also operates at low temperatures [25, 26]. On the other hand, for NiAl and CoTi whose ordering energies are relatively high, ⟨100⟩{011} slip system dominantly operates at all temperatures [27, 28]. Therefore, it is expected that deformation texture of FeAl, NiAl and CoTi developed at high temperature is similar one another because a slip system of ⟨100⟩{011} commonly operates in these three compounds. Indeed, the observed hot-rolling textures of the present compounds are composed of a ⟨111⟩ // ND textural component ({111}⟨uvw⟩) in common.

For NiAl [29, 30] and CoTi [31], it is also known that an additional slip system (i.e., ⟨011⟩{011}) operates at elevated temperatures. However, whether only the slip system of ⟨100⟩{011} (and additional ⟨011⟩{011}) operates during rolling deformation of the present three compounds is not clear at the moment. For Fe_3Al with $D0_3$ or imperfectly B2 structure, rolling texture at elevated temperatures has been simulated using a combination of slip systems, i.e., ⟨111⟩{011}, ⟨111⟩{112}, ⟨111⟩{123}, ⟨100⟩{011} and ⟨011⟩{011} [11–13]. Consequently, the simulated rolling textures of Fe_3Al are best matched with experimental rolling textures when assuming the activation of ⟨111⟩{110} and ⟨111⟩{112} slip systems [11, 13]. These simulations suggest that ⟨100⟩{011} slip system does not contribute so much to formation of rolling texture in the case of Fe_3Al. Therefore, there is a possibility that other slip systems in addition to ⟨100⟩{011} (and ⟨011⟩{011}) operate during rolling deformation of the present three B2 compounds, which result in different rolling textures.

The formed hot-rolling textures are so complex because recrystallization occurs more or less during rolling process for all the compounds. Possibly, the observed hot-rolling textures are affected by repeated rolling deformation and recrystallization. Therefore, the difference in hot-rolling texture among the observed three B2-type compounds is attributed to the activation of additional slip systems such as ⟨011⟩{011} (and ⟨111⟩{110} and/or ⟨111⟩{112}) and/or the introduction of the recrystallization process during hot-rolling (or heating the sheet materials). To clarify the texture development during hot-rolling and annealing of the present intermetallic compounds, more work is required.

3.4. Grain boundary structure

Fig. 5 shows the distribution of grain boundary misorientation angle for Fe-48Al, Ni-50Al and Co-50Ti with fully-recrystallized microstructure whose pole figures are shown in Fig. 4a, e and f. The EBSD measurements were collected at least from different three areas of the specimen. For all the compounds, a significant occurrence (frequency) is found at the misorientation angle of $\sim 5^\circ$. Also, a small and broad peak seems to exist at a misorientation angle of around 45° for all the compounds, similar to the distribution of grain boundary misorientation angle for randomly orientated (textureless) cubic polycrystals [32]. This corresponds with the fact that the observed textures of the present three compounds are relatively weak (Fig. 4a, e and f). In addition, a small peak at a misorientation angle of $\sim 27^\circ$ is recognized for Fe-48Al (Fig. 5a). However, the preferable occurrence of this peak is not explained at the present. Fig. 6 indicates grain boundary character distribution (GBCD) for Fe-48Al, Ni-50Al and Co-50Ti shown in Fig. 5. Irrespective of the kind of compound, the GBCDs are primarily featured by a high frequency ($\sim$15–20%) of $\Sigma 1$ boundaries, i.e.,

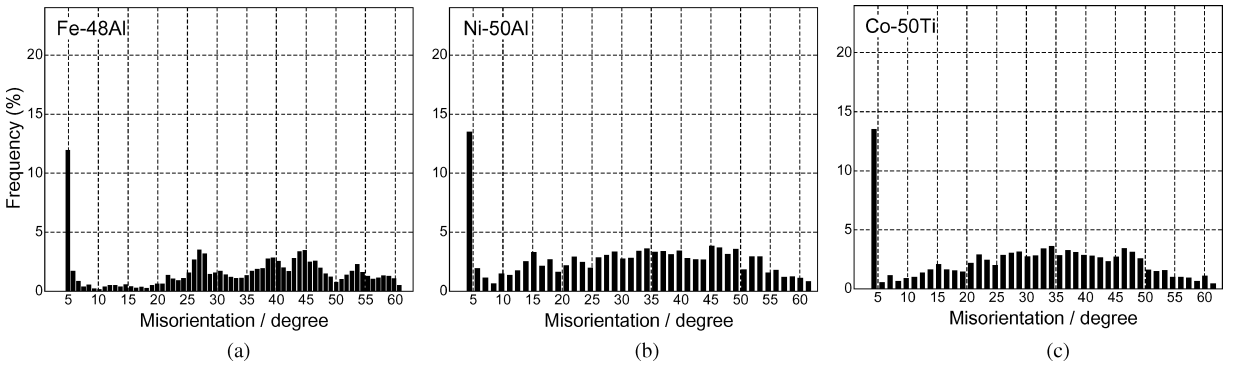

Figure 5 Distribution of grain boundary misorientation for: (a) hot-rolled Fe-48Al, (b) hot-rolled and subsequently annealed Ni-50Al and (c) hot-rolled and subsequently annealed Co-50Ti.

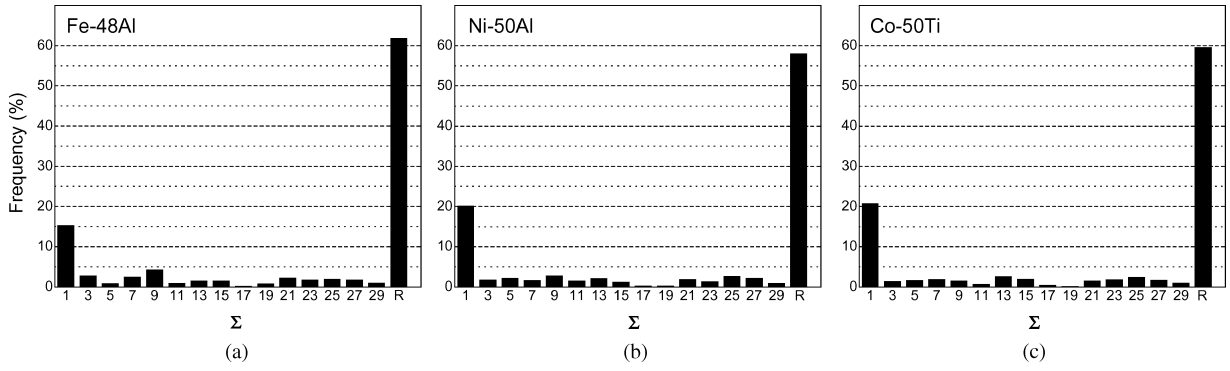

Figure 6 Distribution of grain boundary character for: (a) hot-rolled Fe-48Al, (b) hot-rolled and subsequently annealed Ni-50Al and (c) hot-rolled and subsequently annealed Co-50Ti.

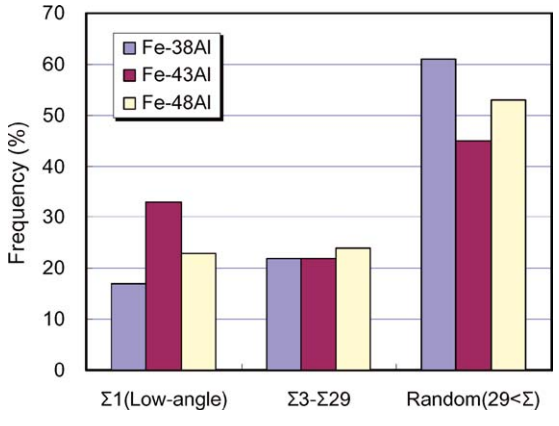

Figure 7 Distribution of grain boundary character for hot-rolled Fe-38Al, -43Al and -48Al.

low-angle boundaries (LABs) besides random (i.e., $29 < \Sigma$) boundaries. No remarkable occurrence of other special (i.e. $\Sigma \leq 29$) boundaries is found in all the compounds. Fig. 7 shows the GBCD of the hot-rolled FeAl as a function of alloy composition (i.e., the Al concentration). In this figure, the type of grain boundaries is divided into three classes, i.e., $\Sigma 1$ (low-angle), $\Sigma 3$-$\Sigma 29$ and random ($29 < \Sigma$) boundaries. The observed GBCD seems to be not so sensitive to alloy composition. Also, the GBCDs shown in Fig. 6 are very similar to those of undeformed (cast and then homogenized) B2-type FeAl with 0.1 at.% Zr and 0.05 at.% B reported by Bystrzycki *et al.* [33]. These results indicate that the GBCD of B2-type intermetallic compounds is little changed by constituent element, alloy composition and processing. As a typical example, the EBSD boundary map of Ni-50Al with a recrystallized microstructure is shown in Fig. 8. In this figure, arrows (broken lines) indicate LABs, i.e., $\Sigma 1$ boundaries. LABs seem to subdivide a coarse grain into smaller grains. A similar structure has been observed for the as-cast B2-type Fe-35Al-4.3Cr-0.1Zr-0.05B (at.%) alloy [33]. For intergranularly brittle intermetallic compounds, LABs (i.e., $\Sigma 1$ boundaries) as well as $\Sigma 3$ twin boundaries are particularly of importance in terms of resistance to cracking (i.e., strong boundary). It has been demonstrated that the LABs and $\Sigma 3$ boundaries

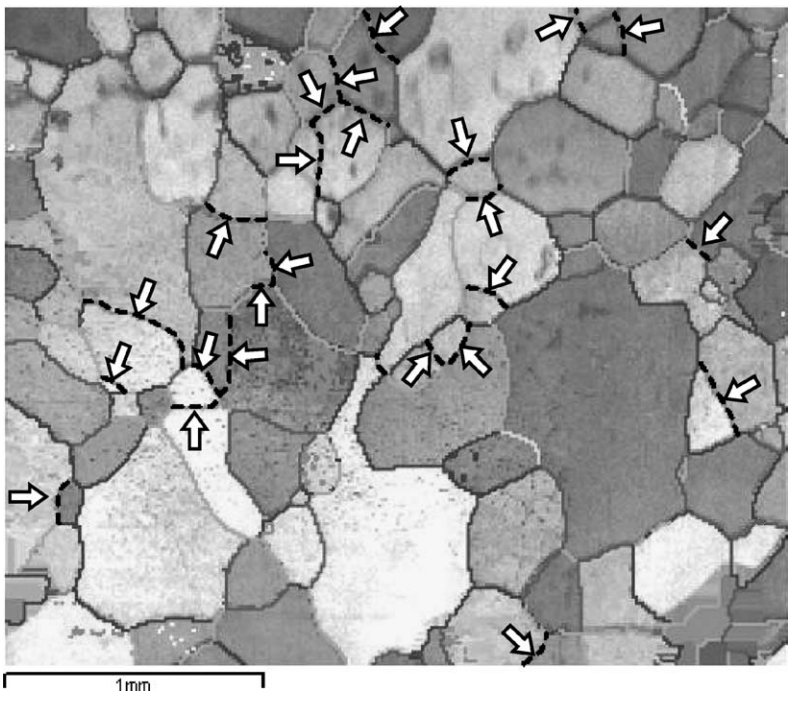

Figure 8 EBSD boundary map of annealed Ni-50Al. Arrows (broken lines) indicate low-angle boundaries (LABs), i.e., $\Sigma 1$ boundaries.

had strong resistivity against intergranular fracture and resulted in high ductility for the $L1_2$-type Ni_3Al and $Ni_3(Al,Ti)$ polycrystalline alloys [34] and also unidirectionally solidified boron-free Ni_3Al polycrystalline [35]. Also for B2-type FeAl, it has been reported that LABs (as well as low Σ boundaries such as $\Sigma 5$ boundaries) show greater crack resistance than other boundaries [32]. Thus, the high frequency of LABs ($\Sigma 1$ boundaries) observed in the present compounds is considered to be favorable in terms of suppression of intergranular fracture.

With respect to other Σ boundaries except for $\Sigma 1$ boundary, the specific interest is paid on $\Sigma 3$ twin boundary which always has the lowest energy minima in the disordered crystal structure. Geometrical consideration of grain boundary structure of $L1_2$ ordered structure reveals that $\Sigma 3$ twin boundary has the crystal structure with no fault energy which is attributed to wrong bonds across a grain boundary [36]. In fact, recrystallized $L1_2$ Co_3Ti [37], Ni_3Al [38] and $Ni_3(Si,Ti)$ [39] ordered alloys with high ordering energy contain many annealing twins and show high frequency of $\Sigma 3$ twin boundaries [38, 40]. On the other hand, the geometrical consideration of grain boundary structure of B2 ordered structure predicts that $\Sigma 3$ twin boundary does not involve the crystal structure with a preferentially low energy level in terms of fault energy [36]. Also, there are not any low Σ boundaries with preferentially low energy level, i.e., energy cusp [36]. Corresponding to this prediction, no significant frequency of special grain boundaries (i.e. $\Sigma \leq 29$) except for $\Sigma 1$ boundary is found in the present compounds.

4. Conclusion

B2-type FeAl, NiAl and CoTi intermetallic compounds were hot-rolled at 1273 K and subsequently annealed at 1273 K for 10 h to investigate workability, texture and grain boundary character distribution as a function of alloy stoichiometry. The following results were obtained:

FeAl was successfully hot-rolled irrespective of alloy stoichiometry. Stoichiometric NiAl and CoTi were also hot-rolled but off-stoichiometric NiAl and CoTi failed.

Hot-rolled FeAl showed a fully-recrystallized microstructure irrespective of alloy stoichiometry. On the contrary, hot-rolled stoichiometric CoTi retained a deformed microstructure. Hot-rolled stoichiometric NiAl retained a partially deformed microstructure. After annealing, both NiAl and CoTi showed fully-recrystallized microstructures, and grain size of annealed NiAl was larger than that of annealed CoTi. These results indicate that recrystallization (and grain growth) occurs easily in the order of FeAl, NiAl and CoTi.

The hot-rolling textures of FeAl, NiAl and CoTi consisted of a ND // {111} textural component in common though the orientation distribution and its intensity were different among these three compounds. By annealing, orientation spread occurred in all the compounds, but the annealing textures were basically similar to the hot-rolling textures. The observed hot-rolling textures were suggested to be governed by recrystallization as well as slip deformation.

The grain boundary character distributions (GBCDs) of the three kinds of compounds with a fully-recrystallized microstructure were similar one another and were characterized by high frequency of $\Sigma 1$ boundaries (i.e., low-angle boundaries).

Acknowledgements

This work was supported in part by the Grant-in-aid for Scientific Research from the Ministry of Education, Culture, Sports and Technology, and by the Light Metal Educational Foundation, Inc., Japan.

References

1. J. L. MURRAY, Bull. Alloy Phase Diagr. **3** (1982) 74.
2. T. TAKASUGI and O. IZUMI, *Phys. Stat. Sol.* (a) **102** (1987) 697.
3. *Idem.*, *J. Mater. Sci.* **23** (1988) 1265.
4. Y. KANENO and T. TAKASUGI, *ibid.* **38** (2003) 869.
5. L. PANG, S. M. HAN and K. S. KUMAR, *Acta Mater.* **50** (2002) 3263.
6. D. LIN, D. LI and Y. LI, *Intermetallics* **6** (1998) 243.
7. D. J. ALEXANDEER, P. J. MAZIASZ and J. L. WRIGHT, *Mater. Sci. Eng.* **A258** (1998) 276.
8. K. E. HARRIS, F. EBRAHIMI and H. GARMESTANI, *ibid.* **A247** (1998) 187.
9. Y. KANENO, T. TAKASUGI and S. HANADA, *ibid.* **A302** (2001) 215.
10. D. G. MORRIS and S. C. DEEVI, *ibid.* **A329–331** (2002) 573.
11. D. RABBE and W. MAO, *Phil. Mag.* A **71** (1995) 805.
12. D. RABBE, J. KEICHEL and Z. SUN, *J. Mater. Sci.* **31** (1996) 339.
13. B. K. KAD, S. E. SCHOENFELD, R. J. ASARO, C. G. MCKAMEY and V. K. SIKKA, *Acta Mater.* **45** (1997) 1333.
14. Y. D. HUANG, W. Y. YANG, G. J. CHEN and Z. Q. SUN, *Intermetallics* **9** (2001) 331.
15. K. E. HARRIS, F. EBRAHIMI and H. GARMESTANI, *Mater. Sci. Eng.* **A247** (1998) 187.
16. D. G. BRANDON, *Acta Metall.* **12** (1966) 1479.
17. M. KOGACHI, S. MINAMIGAWA and K. NAKAHIGASHI, *Acta Metall. Mater.* **40** (1992) 1113.
18. R. NAKAMURA, K. TAKASAWA, Y. YAMAZAKI and Y. IIJIMA, *Intermetallics* **10** (2002) 195.
19. H. NAKAJIMA, W. SPRENGEL and K. NONAKA, *ibid.* **4** (1996) S17.
20. P. NAGPAL and I. BAKER, *Metall. Trans.* **21A** (1991) 2281.
21. M. A. MORRIS, E. P. GEORGE and D. G. MORRIS, *Mater. Sci. Eng.* **A258** (1998) 99.
22. H. XIAO and I. BAKER, *Acta Metal. Mater.* **43** (1995) 391.
23. F. J. HUMPHREYS and M. HATHERLY, in "Recrystallization and Related Annealing Phenomena" (Elsevier Science, Oxford, 1995) p. 49.
24. *Idem.*, *ibid.* p. 335.
25. Y. UMAKOSHI and M. YAMAGUCHI, *Phil. Mag.* A **41** (1980) 573.
26. *Idem.*, *ibid.* **44** (1981) 711.
27. R. D. NOEBE, R. R. BOWMAN and M. V. NATHAL, *Inter. Mater. Rev.* **38** (1993) 193.
28. T. TAKASUGI, K. TSURISAKI, O. IZUMI and S. ONO, *Phil. Mag.* A **61** (1990) 785.
29. J. T. KIM and R. GIBALA, in "High Temperature Ordered Intermetallic Alloy IV Mater. Res. Soc. Symp. Proc," edited by L. Johnson, J.O. Stiegler and D.P. Pope (Materials Research Society, 1991) vol. 213, p. 261.

30. R. D. FIELD, D. F. LAHRMAN and R. DAROLIA, *Acta. Metal. Mater.* **39** (1991) 2951.
31. T. TAKASUGI, M. YOSHIDA and T. KAWABATA, *Phil. Mag. A* **65** (1992) 29.
32. L. C. R. LOPES, C. B. THOMSON and V. RANDLE, *Scripta Mater.* **37** (1997) 1863.
33. J. BYSTRZYCKI, R. A. VARIN, M. NOWELL and K. J. KURZYDLOWSKI, *Intermetallics* **8** (2000) 1049.
34. S. HANADA, T. OGURA, S. WATANABE, O. IZUMI and T. MASUMOTO, *Acta Metal.* **34** (1986) 13.
35. T. WATANABE, T. HIRANO, T. OCHIAI and H. OIKAWA, *Mater. Sci. Forum* **157–162** (1994) 1103.
36. T. TAKASUGI and O. IZUMI, *Acta Metal.* **31** (1983) 1187.
37. Y. KANENO, I. NAKAAKI and T. TAKASUGI, *J. Mater. Res.* **17** (2002) 2567.
38. N. MASAHASHI and S. HANADA, *Z. Metallkd.* **91** (2000) 516.
39. Y. KANENO, I. NAKAAKI and T. TAKASUGI, *Intermetallics* **10** (2002) 693.
40. Y. KANENO and T. TAKASUGI, *Met. Mater. Trans.* **34A** (2003) 2429.

Received 2 May 2003
and accepted 20 September 2004